Protein Science (1999), *8*:934–940. Cambridge University Press. Printed in the USA.

ACCELERATED COMMUNICATION

Carbamate kinase: New structural machinery for making carbamoyl phosphate, the common precursor of pyrimidines and arginine

ALBERTO MARINA,[1] PEDRO M. ALZARI,[2] JERÓNIMO BRAVO,[3] MATXALEN URIARTE,[1] BELÉN BARCELONA,[1] IGNACIO FITA,[3] AND VICENTE RUBIO[1]

[1]Instituto de Biomedicina de Valencia (CSIC), C/Jaime Roig 11, Valencia 46010, Spain
[2]Unité de Biochimie Structurale, URA CNRS 1961, Institut Pasteur, 25 rue du Dr. Roux, 75724 Paris Cedex 15, France
[3]CID-CSIC, C/Jordi Girona 18-26, Barcelona 08034, Spain

(RECEIVED December 16, 1998; ACCEPTED January 4, 1999)

Abstract

The enzymes carbamoyl phosphate synthetase (CPS) and carbamate kinase (CK) make carbamoyl phosphate in the same way: by ATP-phosphorylation of carbamate. The carbamate used by CK is made chemically, whereas CPS itself synthesizes its own carbamate in a process involving the phosphorylation of bicarbonate. Bicarbonate and carbamate are analogs and the phosphorylations are carried out by homologous 40 kDa regions of the 120 kDa CPS polypeptide. CK can also phosphorylate bicarbonate and is a homodimer of a 33 kDa subunit that was believed to resemble the 40 kDa regions of CPS. Such belief is disproven now by the CK structure reported here. The structure does not conform to the biotin carboxylase fold found in the 40 kDa regions of CPS, and presents a new type of fold possibly shared by homologous acylphosphate-making enzymes. A molecular 16-stranded open β-sheet surrounded by α-helices is the hallmark of the CK dimer. Each subunit also contains two smaller sheets and a large crevice found at the location expected for the active center. Intersubunit interactions are very large and involve a central hydrophobic patch and more hydrophilic peripheral contacts. The crevice holds a sulfate that may occupy the site of an ATP phosphate, and is lined by conserved residues. Site-directed mutations tested at two of these residues inactivate the enzyme. These findings support active site location in the crevice. The orientation of the crevices in the dimer precludes their physical cooperation in the catalytic process. Such cooperation is not needed in the CK reaction but is a requirement of the mechanism of CPSs.

Keywords: carbamate kinase; carbamoyl phosphate synthetase; crystal structure; dimeric enzymes; phase extension; selenomethionine substitution; subunit interface

Carbamoyl phosphate (CP) synthesis is crucial for life, because pyrimidines, arginine, and urea derive from carbamoyl phosphate made by carbamoyl phosphate synthetase (CPS). The CPS from *Escherichia coli* is a heterodimer of 40 and 120 kDa subunits of which the larger subunit catalyzes the full reaction from ATP, bicarbonate, and ammonia (Meister, 1989). A simpler enzyme, carbamate kinase (CK), consisting of a homodimer of a 33 kDa subunit, also makes CP in the presence of ATP, bicarbonate, and ammonia (Marshall & Cohen, 1966; Marina et al., 1998). However, the true substrate of CK is carbamate generated chemically from bicarbonate and ammonia, and the equilibrium favors CP utilization (Jones & Lipmann, 1960; Marshall & Cohen, 1966). Nevertheless, an enzyme resembling CK in molecular properties and amino acid sequence is used to synthesize CP in hyperthermophylic archea (Purcarea et al., 1996; Durbecq et al., 1997). Ultimately, CK and CPS make CP in the same way: by phosphorylating carbamate in an identical ATP-dependent reaction (Rubio, 1993; Rubio et al., 1998). However, CPS uses an extra ATP molecule to synthesize carbamate by phosphorylating bicarbonate in a reaction that is formally analogous to the phosphorylation of carbamate, followed by reaction of the resulting carboxyphosphate with ammonia (Rubio et al., 1998). CK also catalyzes, although with low efficiency, the phosphorylation of bicarbonate (Marina et al., 1998). Thus, CK can catalyze the two phosphorylation steps of the CPS reaction, and CPS might be a modified CK in which the two CK monomers have been fused into a single polypeptide, and each monomer carries out a different phosphorylation step (Rubio,

Reprint requests to: Vicente Rubio, Instituto de Biomedicina, C/Jaime Roig 11, Valencia 46010, Spain; e-mail: rubio@ibv.csic,es.

Abbreviations: BC, biotin carboxylase; CK, carbamate kinase; CPS, carbamoyl phosphate synthetase; CP, carbamoyl phosphate.

1993; Durbecq et al., 1997). This agrees with the finding of internal sequence homology (Nyunoya & Lusty, 1983) and a pseudohomodimeric organization in CPS (Thoden et al., 1997; Rubio et al., 1991). In the recently determined three-dimensional structure of *E. coli* CPS (Thoden et al., 1997), the two domains involved in the phosphorylation of bicarbonate and carbamate are structurally very similar and also closely resemble the structure of biotin carboxylase (BC) (Waldrop et al., 1994), a component of biotin enzymes that also makes carboxyphosphate from ATP and bicarbonate (Climent & Rubio, 1986). The BC fold is also found in other ADP-forming ligases such as glutathione synthetase and D-Ala:D-Ala ligase (Artymiuk et al., 1996), and consists of three domains with central open β-sheets and characteristic topologies of the secondary structure elements. Given the similarities in the reactions catalyzed by CPS and CK, it was expected that the structure of the latter would also include the BC fold. However, the crystal structure of CK reported here does not support this expectation: the enzyme has an α/β fold that is not found in other enzymes of known structure. Structural determination was carried out at 2.8 Å resolution by multiple isomorphous replacement using thimerosal and $(Ta_6Br_{12})^{2+}$ derivatives, and density modification techniques (Table 1). In the present refined model, the three C-terminal residues are not included, and only Tyr233, Thr247, and Met298, all of them in poorly ordered loops, are in the disallowed regions of the Ramachandran plot. Replacement of methionines by selenomethionine helped sequence assignment.

Overall structure

In agreement with previous data (Bishop & Grisolia, 1966; Marshall & Cohen, 1966; Marina et al., 1998), CK was found to be a dimer of identical subunits (Figs. 1, 2). Approximate dimer dimensions are 100 × 50 × 45 Å. Each subunit is split by a large crevice in N- and C-terminal regions consisting of residues Gly2–Val220 (Met1 is removed post-translationally; Marina et al., 1998) and Asp221–Lys310, respectively. The organization in the dimer of the C- and N-regions is C-N*N′-C′. The N-terminal region is the central part of the dimer, providing the entire intersubunit interface. This region contains (Fig. 3A): (1) a four-stranded parallel β-sheet (β1, β2, β3, and β9) surrounded by α-helices αA, αB, and αC on one side and αE and αF on the other side of the sheet; (2) a smaller four-stranded mixed β-sheet (β4, β8, β10, and β11; see right-hand monomer in Fig. 1B); and (3) a protruding subdomain that hangs over the crevice (Figs. 1B, 2) and that consists of residues 130–160 forming a three-stranded antiparallel sheet (β5, β6, and β7) and one α-helix (αD). The C-terminal portion contains a mixed four-stranded β-sheet (β12, β13, β14, and β15; see Fig. 1A), surrounded by αG, αH, and αI, and an exposed loop (Leu228–Leu246) joining β12 and β13 that participates in crystal contacts and presents some disorder. The β-sheet of the C-region and the parallel sheet of the N-region form together an eight-stranded sheet via parallel hydrogen bonding of β12 with β1 (Figs. 2A, 3A). In turn, a 16-stranded open molecular β-sheet that is the hallmark of the molecule is formed by the two eight-stranded β-sheets of the subunits via antiparallel hydrogen bonding of the β3 strands at the dimer interface, with an angle between the strands of 120° (Fig. 1A,B). The hydrogen bonds between the main-chain atoms of strands β3 extend by including fixed water molecules that bridge the two subunits (Fig. 1B, part 3). In addition to the interactions of β3, the dimer interface involves interactions of αB and αC (labeled in the left-hand monomer of Fig. 1B) with the same elements of the other subunit. Leu60, Met81, Tyr88, and Leu111 contribute large contact areas. Residues toward the N-terminus of αC provide the central part of the surface of interaction, which is strongly hydrophobic and includes the sulfur-containing residues Met73, Cys78, and Met81. These residues proved highly valuable in the confirmation of the fitting of the sequence to the electron density map thanks to the replacement of the methionines by selenomethionine or the formation of a thimerosal complex with the cysteine (Fig. 1B, part 2). In contrast to the interaction surface provided by β3 and αC, which is relatively flat and perpendicular to the major molecular axis, αB, and the loop connecting it to αC

Table 1. *Data collection and refinement statistics*

Diffraction data and MIR phasing	Resolution (Å)	No. of reflections (% completeness)	$\langle I/\sigma_I \rangle$	Mult	R_{merg}	R_{iso}	Sites	Phasing power	R_{cullis}	FOM[a]
Native	15–2.8	31,935 (89.5)	8.9	3.1	0.064					
Thimerosal	24–2.9	31,892 (96.8)	5.7	3.3	0.127	0.282	7	1.02	0.86	0.25
$(Ta_6Br_{12})^{2+}$	19–3.0	28,431 (99.0)	7.0	3.2	0.100	0.386	2	1.60[b]	0.72[b]	0.34[b]
Selenomethionine	15–3.0	27,492 (96.6)	6.6	3.0	0.105	0.251	24[c]	NU[d]	NU	NU

Refined model			
Resolution	15–2.8 Å	Disordered residues	308–310
R-factor	22.4	No. of residues in asymmetric unit	1,226
R_{free}	28.3	No. of sulfate molecules	4
RMS deviation in bonds	0.005 Å	No. of solvent molecules	64
RMS deviation in angles	1.4°	Total No. of non-H atoms	9,157
RMS deviations in temperature	2.6 Å^2	Anisotropic correction (a^*; b^*; c^*)	−29 Å^2, 13 Å^2, −4 Å^2
		Average *B*-factor	28 Å^2

[a] FOM = figure of merit.
[b] Resolution between 15 and 6 Å.
[c] All six methionines were replaced by selenomethionine in each monomer (see text). However, of the 24 selenium atoms, only 16 were located in difference Fourier maps.
[d] NU = not used.

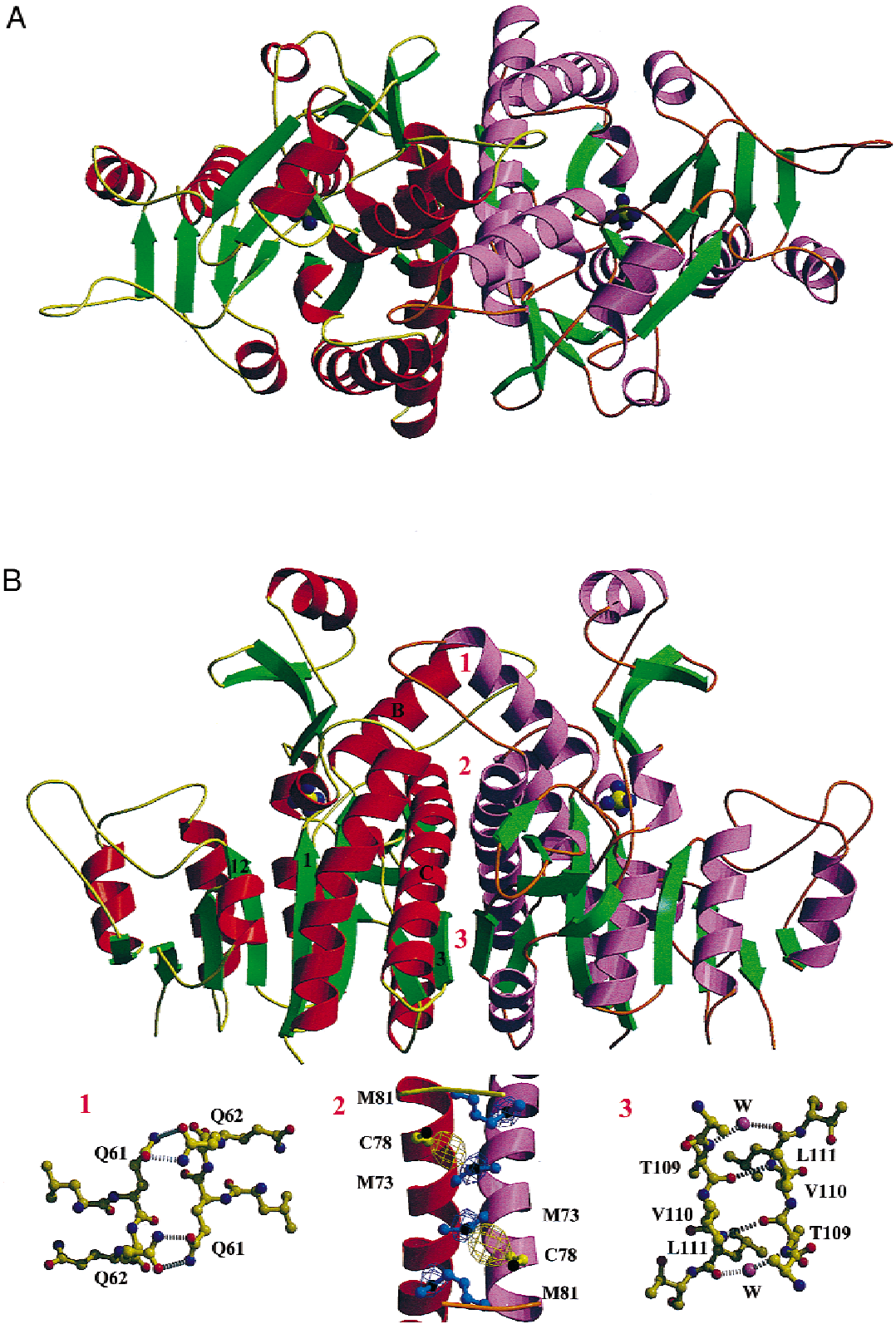

Fig. 1. Ribbon representation of CK with views (**A**) down and (**B**) perpendicular to the molecular twofold axis. Helices are shown in purple and strands in green. Different color tones are used for the two subunits. The bound sulfates are shown in space-filling representation. In (**B**) figures and letters in the left-hand monomer denote β-strands 1, 3, and 12, and α-helices B and C. The figures at the intersubunit interface mark the regions shown in detail in the corresponding panels at the bottom. Panel 1: complementary hydrogen bonds between Gln61 and Gln62 in the helix B region of the interface. Panel 2: central region of the interface (helix C), detailing in ball-and-stick representation methionines 73 and 81 (in blue) and cysteine 78 (in green), with sulfur atoms in black. The orientation follows down the molecular twofold axis. Difference electron density maps between the native CK and the selenomethionine and thimerosal derivatives are displayed in blue and yellow, respectively, confirming the sequence assignment. Panel 3: main-chain hydrogen bonds between strands β3 showing two bridging fixed water molecules (W).

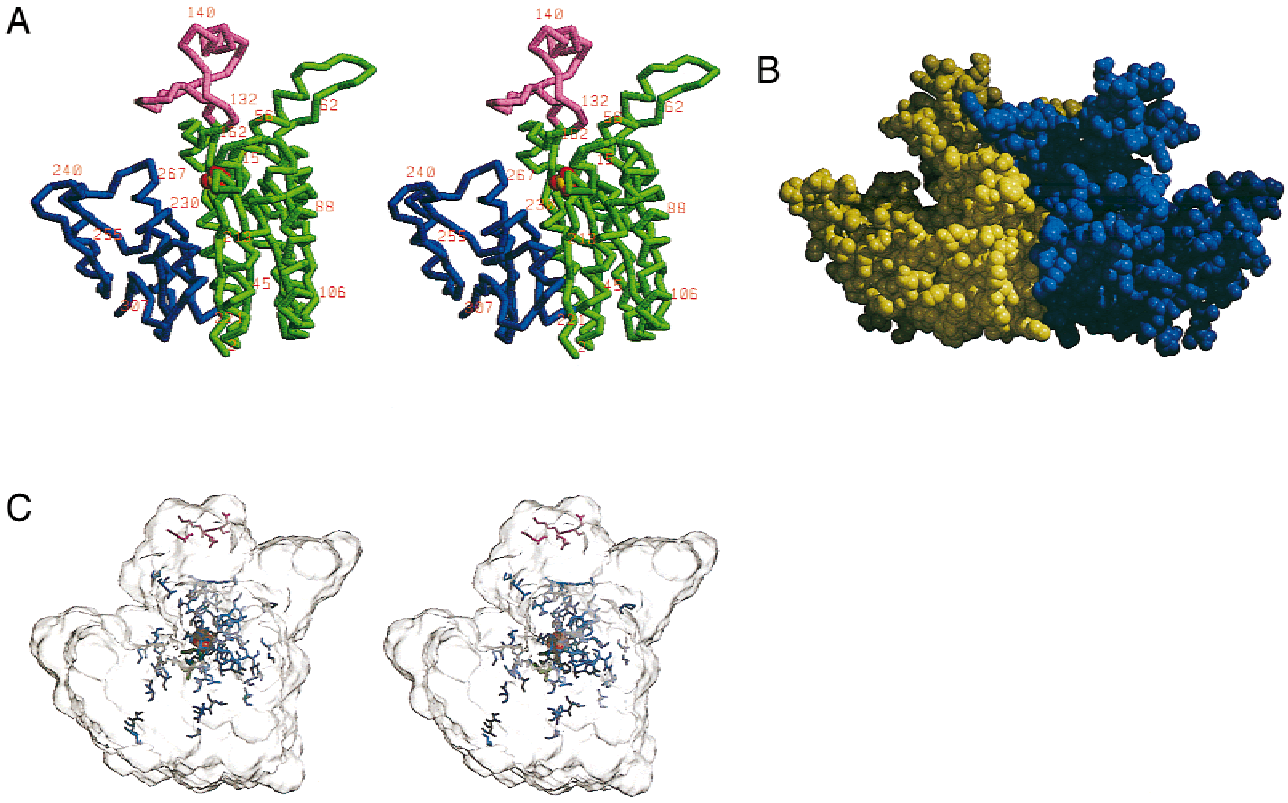

Fig. 2. A: Stereo view of the backbone of one subunit of CK, oriented as the left-hand subunit of Figure 1B. The protruding subdomain is colored magenta and the N- and C-terminal regions in green and blue, respectively. The sulfate is shown with a space-filling representation. **B:** Space-filling model of the CK dimer in the same orientation. **C:** Transparent surface representation of one subunit of CK with similar orientation to that in **A**, showing in green Asp208 and Asp210; in blue other conserved residues; and in magenta Glu136, Glu138, Glu141, and Lys140.

protrude obliquely toward the other monomer across the intersubunit plane providing a safety closure mechanism (Fig. 1A,B) that involves double hydrogen bonds between the side-chain amido groups of Gln61 and Gln62 from the two subunits (Fig. 1B, part 1). Overall the interactions across the dimer interface appear to be hydrophobic in a central area (helix C) and more hydrophilic in the periphery (helix B and strand β3), with a total buried area, measured with a probe radius of 1.7 Å, of 3,700 Å^2, with about 1,500 Å^2 corresponding to hydrophobic groups. The extension and nature of the interactions can explain the high stability of the dimer.

Putative active center

The crevice between the N- and C-terminal regions is the only large pocket found in the structure (Fig. 2B), and its localization is characteristic of catalytic centers in open α/β structures (Bränden, 1980), being at the COOH-end of adjacent, nonconsecutive, oppositely connected, parallel β-strands (β1 and β12). The crevice is extended by a wall formed by the mixed, four-stranded β-sheet of the N region, and the protruding subdomain hangs over it as a lid (Figs. 1, 2). A strong peak of electron density is found at the bottom of the crevice, and is interpreted to correspond to a bound sulfate (Fig. 3B). Sulfate present in crystallization solutions was reported with other enzymes (Alexeev et al., 1994) to occupy the site of a phosphate from the substrate ATP. Charge distribution, estimated with the program GRASP, and steric analysis are compatible with the binding in the crevice of an extended ATPMg molecule. The formation of a strong bond between the sulfate and Gly11 is revealed by the continuity of their electron densities (Fig. 3B). Glycine residues are generally found in loops involved in binding the polyphosphate chain of ATP (Schultz, 1992). Gly11 is part of the β1-αA loop (residues 10–14), apparently a functionally important loop, given its strict sequence conservation in all known CKs (Marina et al., 1998). In fact, most conserved residues in CK sequences line the crevice (Fig. 2C). When two such residues, Asp208 and Asp210, were replaced by alanine, the activity of the soluble and partially purified mutant enzymes was only about 0.1% that of the wild-type enzyme. In contrast, replacement by alanine of glutamates 136, 138, and 141 and of lysine 140 (Fig. 2C), four charged nonconserved residues that do not line the crevice, was not detrimental. All the above information provides strong evidence for the location of the active center at the crevice of each subunit. The orientation of the crevices in the dimer precludes their catalytic cooperation or the migration of intermediates between them. Such cooperation is not needed in the CK reaction (Marshall & Cohen, 1966), but is a requisite of the three-step mechanism of CPSs (Rubio et al., 1998). A tunnel exists in the structure of CPS joining the two phosphorylating centers (Thoden et al., 1997). No such tunnel is found in the structure of CK, and therefore, it is difficult to reconcile the reported CPS activity of the CK-like CPS of *Pyrococcus furiosus* (Durbecq et al., 1997; Marina et al., 1998) with the present structure. Thus, either the subunits of

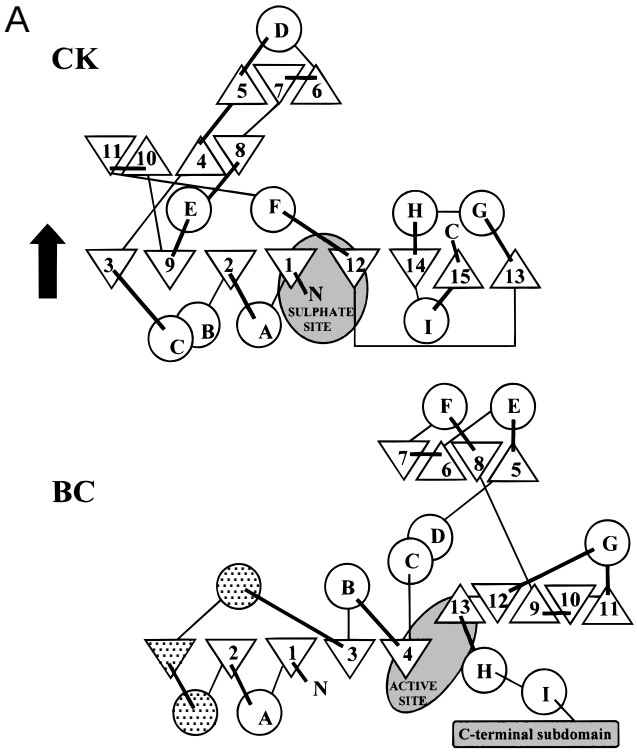

Fig. 3. A: Topology of secondary structure elements (circles, α-helices; triangles, β-strands) of the CK monomer (CK), compared with that of the BC fold (taken from Artymiuk et al., 1996) as it appears in BC and CPS. Elements that are not constant in other proteins of the the BC family are shadowed. The active center location in BC is that given in Artymiuk et al. (1996). The molecular binary axis in CK is indicated with an arrow. Structural assignments in the topology of CK are as follows: residues 3 to 10 (β1), 21 to 41 (αA), 43 to 51 (β2), 52 to 65 (αB), 75 to 101 (αC), 106 to 110 (β3), 113 to 116 (β4), 128 to 131 (β5), 136 to 144 (αD), 148 to 152 (β6), 156 to 161 (β7), 166 to 169 (β8), 172 to 180 (αE), 183 to 186 (β9), 193 to 196 (β10), 201 to 203 (β11), 209 to 220 (αF), 224 to 229 (β12), 247 to 250 (β13), 251 to 259 (αG), 268 to 280 (αH), 286 to 290 (β14), 292 to 297 (αI), and 302 to 306 (β15). **B:** Stereo views of the averaged ($2F_o - F_c$) electron density map of the sulfate anion and surrounding residues. The molecular model of the corresponding residues is superimposed. Broken bonds correspond to hydrogen bridges. All residues shown except Leu15 are highly conserved in CK sequences. The views in the upper and lower panels are rotated around the *y* axis by 90° with respect to each other. This rotation results in the clustering of residues at the left of the sulfate in the view shown in the lower panel; therefore, for clarity, only Gly11 and His49 are indicated among these clustered residues.

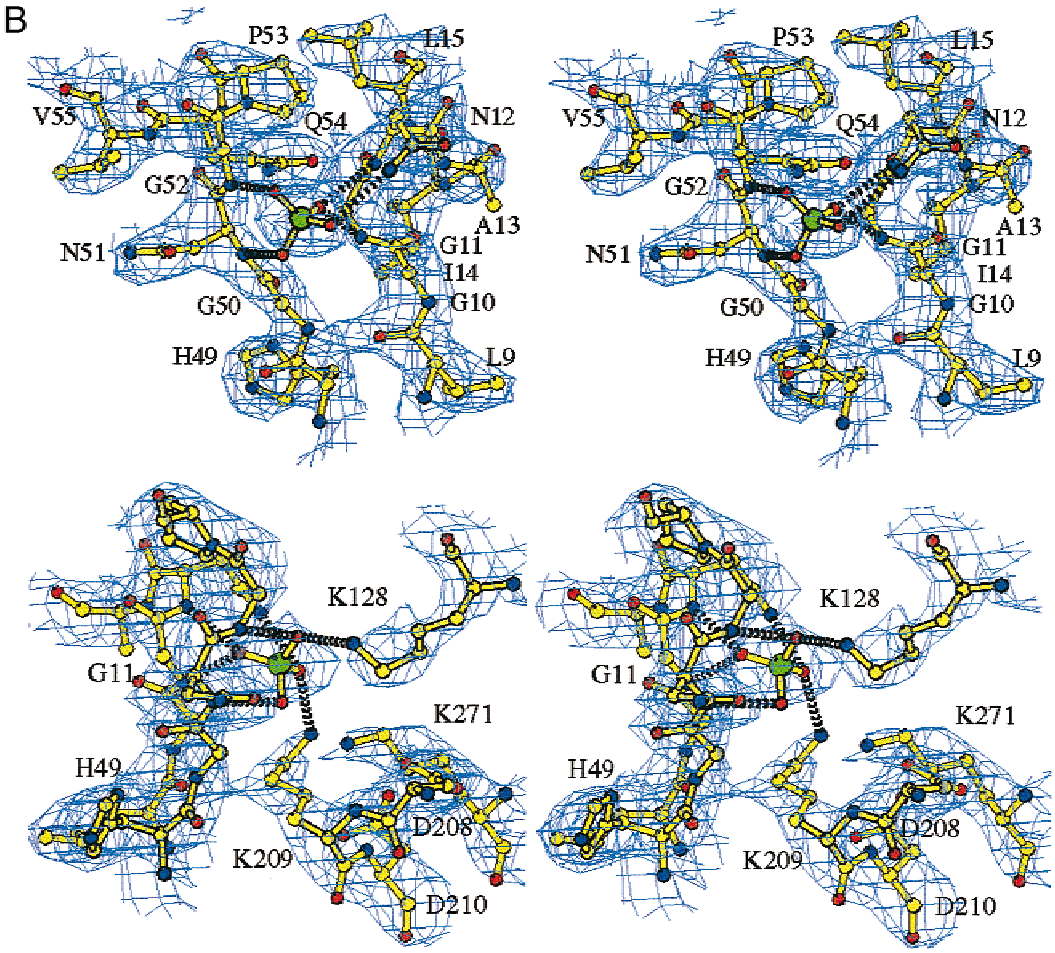

the pyrococcal enzyme dimerize differently than the CK studied here or the identification of the *P. furiosus* enzyme as CPS rather than CK has to be re-examined.

Structural comparisons (Fig. 3A)

The CK structure is different from that of the BC fold found in the carbamate phosphorylating domain of CPS (Thoden et al., 1997), the CPS domain that catalyzes the same reaction as CK. Although both structures have parallel open β-sheets surrounded by α-helices on both sides, forming a modified "Rossmann fold," the number of parallel strands is greater in CK and the order of secondary structure elements in the sequence differs widely in the two structures. Thus, the BC fold has, ordered from N to C terminus, three self-contained domains with central open sheets and single connections with the adjacent domains (Artymiuk et al., 1996). In contrast, three of the four β-sheets of CK are nested within each other, and one of them makes four external connections. Use of the DALI package (Holm & Sander, 1993) failed to reveal significant structural similarities of CK with other known protein structures, other than those due to the presence of the modified "Rossmann fold." Thus, CK appears to represent a new structural variant among the family of open sheet α/β proteins, a fold that may be shared by other acylphosphate-forming enzymes shown to have sequence homology with CK, such as N-acetyl glutamate kinase, γ-glutamyl kinase, and long chain fatty acyl CoA-synthetase (Marina et al., 1998). The structural comparison with the CK-like CPS of *P. furiosus* will also be interesting, not only for the perplexing mechanistic questions raised, but also because of the extreme thermostability of the pyrococcal enzyme ($t_{1/2}$ of approximately 30 min at 100 °C; Durbecq et al., 1997), whereas CK is unstable above 55 °C (Marina et al., 1998). Current efforts in our laboratory are directed to determine the structure of this enzyme.

Materials and methods

Orthorhombic crystals of CK purified from *Enterococcus faecium* (Marina et al., 1994) diffracted at least to 2.5 Å resolution (synchrotron radiation). Space group was $P2_12_12_1$ and unit cell dimensions $a = 82.9$ Å, $b = 172.9$ Å, and $c = 98.8$ Å. Data collected at vapor–liquid nitrogen temperature on a MARRESEARCH imaging plate were processed using DENZO and SCALEPACK (Otwinowski, 1993) (Table 1). Four CK monomers were estimated per asymmetric unit. Crystal soaking was used to obtain heavy atom derivatives $(Ta_6Br_{12})^{2+}$ (Knäblein et al., 1997) or thimerosal. Two $(Ta_6Br_{12})^{2+}$ clusters with different relative occupancies were located in the asymmetric unit. Rotational disorder within each cluster (Löwe et al., 1995) prevented the obtaining of good SIR phasing beyond 6 Å resolution. This initial phasing identified, by difference Fourier synthesis, seven mercury atoms in the thimerosal derivative. The combined phases at 3.0 Å resolution were improved with a density modification protocol starting at 6.5 Å resolution and using only solvent-flattening restrictions (Cowtan & Main, 1993). The resulting map at 4.0 Å resolution was used to determine the position of the noncrystallographic symmetry elements with AMORE (Navaza, 1994; Domínguez et al., 1995), showing that the four monomers in the asymmetric unit were as a pair of dimers. Each dimer subunits are related by a diad axis, and the two dimers are related by a noncrystallographic translational symmetry operation. Molecular envelopes were automatically determined as the points where the electron density gave high correlation after applying the noncrystallographic symmetry operation (CORMAP program; P.M. Alzari, unpubl. obs.). The phase extension process was repeated, starting again at 6.5 Å resolution, simultaneously taking into account the restraints imposed by solvent flattening and by the fourfold noncrystallographic symmetries (Rossman, 1990). The resulting map at 3 Å resolution allowed model building of about 60% of the CK polypeptide. Phase information derived from this partial model was combined using SIGMAA (Read, 1986) with the original multiple isomorphous replacement phases and the density modification process was repeated again. Most of the sequence was assigned in the resulting map at 2.8 Å resolution, although residues 233–262 and 294–302 were still poorly defined. Refinement and rebuilding with X-PLOR (Brünger, 1992a) and O (Jones et al., 1991), respectively, gave the present molecular model, which includes residues Gly2 to Val307, one sulfate anion and 16 well-defined water molecules per subunit, with an *R*-factor of 22.4% and an R_{free} of 28.3% when solvent corrections and overall anisotropic *B*-factor scaling were used (Table 1). The R_{free} criterion (Brünger, 1992b) was used during all the model-building and refinement steps. The fourfold redundancy of the noncrystallographic symmetry was used as a tight restraint throughout all the refinement and map averaging steps. These restraints were released for residues 233–262 during the final cycles of refinement because this region presented significant deviations from the strict noncrystallographic symmetry, likely due to differences in crystal contacts. These differences are also reflected in the average temperature factors of the polypeptide backbones, which are 23 and 25 Å^2 for the monomers in one dimer and 31 and 34 Å^2 in the other. Residues 297–301 form a short exposed loop that appears flexible, and is poorly defined.

To prepare selenomethionine-containing CK, the enzyme was expressed from the enterococcal gene, cloned in plasmid pCK41 (Marina et al., 1998), using a methionine auxotroph (*E. coli* B834 (DE3)pLysS; from Novagen, Madison, Wisconsin) in methionine-free medium containing 50 mg L^{-1} L-selenomethionine (Budisha et al., 1995) (obtained from Sigma, St. Louis, Missouri). All six methionines of the CK monomer were replaced by selenomethionine, as shown by mass spectrometry, but only four yielded strong peaks in the different Fourier maps with respect to natural CK, confirming the location of the sulfur atoms of 16 of the 24 methionines in the asymmetric unit (Fig. 1B, part 2). The seven mercury atoms found in the thimerosal derivative were localized near the side chains of cysteine residues 78 and 235.

CK, with the multiple mutations D208A-D210A or E136A-E138A-K140A-E141A, was prepared by site-directed mutagenesis of pCK41 (Marina et al., 1998) using a double PCR procedure (Barettino et al., 1994). The mutations were confirmed by restriction analysis and DNA sequencing. The mutant enzymes were prepared and assayed as reported (Marina et al., 1998).

Coordinates

Atomic coordinates and structure factors for carbamate kinase have been deposited with the Protein Data Bank with accession codes 1b7b and r1b7bsf, respectively.

Acknowledgments

We thank E. Giralt for mass spectrometry, R. Huber, and X. Gomis-Rüth for supplying $(Ta_6Br_{12})^{2+}$, A. Guarné and A. González for assistance on the EMBL beamline at the DESY synchrotron, and W. Mellik-Adams, D.

Stuart, and J. Tormo for valuable discussions. This work was supported by grants PB95-0218 and PM97-0134-CO2-01 of the Dirección General de Enseñanza Superior (DGES) of Spain. Data collection in the synchrotron was supported by the Human Capital and Mobility Programme of the European Union. A. Marina, B. Barcelona, and M. Uriarte were fellows, respectively, of the Valencian and Spanish Governments and of Bancaixa-FVIB. A. Marina was also a short-term fellow of EMBO.

References

Alexeev D, Baxter RL, Sawyer L. 1994. Mechanistic implications and family relationships from the structure of dethiobiotin synthetase. *Structure 2*:1061–1072.

Artymiuk PJ, Poirrette AR, Rice DW, Willett P. 1996. Biotin carboxylase comes into the fold. *Nat Struct Biol 3*:128–132.

Barettino D, Feigenbutz M, Valcárcel R, Stunnenberg HG. 1994. Improved method for PCR-mediated site-directed mutagenesis. *Nucleic Acids Res 22*:541–542.

Bishop SH, Grisolia S. 1966. Crystalline carbamate kinase. *Biochim Biophys Acta 118*:211–218.

Bränden CI. 1980. Relation between structure and function of α/β proteins. *Q Rev Biophys 13*:317–338.

Brünger AT. 1992a. *X-PLOR: Version 3.1. A system for X-ray crystallography and NMR*. New Haven, Connecticut: Yale University Press.

Brünger AT. 1992b. Free *R*-value: Novel statistical quantity for assessing the accuracy of crystal structures. *Nature 355*:472–475.

Budisha N, Steipe B, Denange P, Eckerskorn C, Kellermann J, Huber R. 1995. High-level biosynthetic substitution of methionine in proteins by its analogs 2-aminohexanoic acid, elenomethionine, telluromethionine and ethionine in *Escherichia coli*. *Eur J Biochem 230*:788–796.

Climent I, Rubio V. 1986. ATPase activity of biotin carboxylase provides evidence for initial activation of HCO_3^- by ATP in the carboxylation of biotin. *Arch Biochem Biophys 251*:465–470.

Cowtan KD, Main P. 1993. Improvement of macromolecular electron-density maps by the simultaneous application of real and reciprocal space constraints. *Acta Crystallogr A49*:148–157.

Domínguez R, Souchon H, Spinelli S, Dauter Z, Wilson KS, Chauvaux S, Béguin P, Alzari PM. 1995. A common protein fold and similar active site in two distinct families of beta-glycanases. *Nat Struct Biol 2*:569–576.

Durbecq V, Legrain C, Roovers M, Pierard A, Glansdorff N. 1997. The carbamate kinase-like carbamoyl phosphate synthetase of the hyperthermophilic archeon *Pyrococcus furiosus*, a missing link in the evolution of carbamoyl phosphate biosynthesis. *Proc Natl Acad Sci USA 94*:12803–12808.

Holm L, Sander C. 1993. Protein structure comparison by alignment of distance matrices. *J Mol Biol 233*:123–138.

Jones ME, Lipmann F. 1960. Chemical and enzymatic synthesis of carbamyl phosphate. *Proc Natl Acad Sci USA 46*:1194–1205.

Jones TA, Zou JY, Cowan SW, Kjeldgaard M. 1991. Improved methods for building protein models in electron density maps and the location of errors in these models. *Acta Crystallogr A47*:110–119.

Knäblein J, Neuefeind T, Schneider F, Berger A, Messerchmidt A, Löwe J, Steipe B, Huber R. 1997. $(Ta_6Br_{12})^{2+}$ a tool for phase determination of large biological assemblies by X-ray crystallography. *J Mol Biol 270*:1–7.

Löwe J, Stock D, Jap B, Zwicki P, Baumeister W, Huber R. 1995. Crystal structure of the 20S proteasome from the Archaeon *T. acidophilum* at 3.4 Å resolution. *Science 269*:533–539.

Marina A, Bravo J, Fita I, Rubio V. 1994. Crystallization, characterization and preliminary crystallographic studies of carbamate kinase of *Streptococcus faecium*. *J Mol Biol 235*:1345–1347.

Marina A, Uriarte M, Barcelona B, Fresquet V, Cervera J, Rubio V. 1998. Carbamate kinase from *Enterococcus faecalis* and *Enterococcus faecium*. Cloning of the genes, studies on the enzyme expressed in *Escherichia coli*, and sequence similarity with N-acetyl-L-glutamate kinase. *Eur J Biochem 253*:280–291.

Marshall M, Cohen PP. 1966. A kinetic study of the mechanism of crystalline carbamate kinase. *J Biol Chem 241*:4197–4208.

Meister A. 1989. Mechanism and regulation of the glutamine-dependent carbamyl phosphate synthetase of *Escherichia coli*. *Adv Enzymol Relat Areas Mol Biol 62*:315–374.

Navaza J. 1994. AMoRe: An automated package for molecular replacement. *Acta Crystallogr A50*:157–163.

Nyunoya H, Lusty CJ. 1983. The carB gene of *Escherichia coli*: A duplicated gene coding for the large subunit of carbamyl-phosphate synthetase. *Proc Natl Acad Sci USA 80*:4629–4633.

Otwinowski Z. 1993. Oscillation data reduction program. In: Sawyer L, Isaccs N, Bailey S, eds. *Data collection and processing*. Warrington, UK: SERC Daresbury Laboratory. p 56.

Purcarea C, Simon V, Prieur D, Hervé G. 1996. Purification and characterization of carbamoyl-phosphate synthetase from the deep-sea hyperthermophilic archaebacterium *Pyrococcus abyssi*. *Eur J Biochem 236*:189–199.

Read R. 1986. Improved Fourier coefficients for maps using phases from partial structures with errors. *Acta Crystallogr A42*:140–149.

Rossman MG. 1990. The molecular replacement method. *Acta Crystallogr A46*:73–82.

Rubio V. 1993. Structure–function studies in carbamoyl phosphate synthetases. *Biochem Soc Transact 21*:198–202.

Rubio V, Cervera J, Lusty CJ, Bondala E, Britton HG. 1991. Domain structure of the large subunit of *Escherichia coli* carbamoyl phosphate synthetase. Location of the binding site for the allosteric inhibitor UMP in the COOH-terminal domain. *Biochemistry 30*:1068–1075.

Rubio V, Llorente P, Britton HG. 1998. Mechanism of carbamoyl phosphate synthetase from *Escherichia coli*. Binding of the ATP molecules used in the reaction and sequestration by the enzyme of the ATP molecule that yields carbamoyl phosphate. *Eur J Biochem 255*:262–270.

Schultz GE. 1992. Binding of nucleotides by proteins. *Curr Opin Struct Biol 2*:61–67.

Thoden JB, Holden HM, Wesenberg G, Raushel FM, Rayment I. 1997. Structure of carbamoyl phosphate synthetase: A journey of 96 Å from substrate to product. *Biochemistry 36*:6305–6316.

Waldrop GL, Rayment I, Holden HM. 1994. Three-dimensional structure of the biotin carboxylase subunit of acetyl-CoA carboxylase. *Biochemistry 33*:10249–10256.